

IN SITU INVESTIGATION OF THE EFFECTS OF GRAVITY LEVEL VARIATIONS ON THE DIRECTIONAL SOLIDIFICATION MICROSTRUCTURES DURING PARABOLIC FLIGHTS

L. Abou-Khalil¹, G. Salloum-Abou-Jaoude², G. Reinhart¹, C. Pickmann³,
G. Zimmermann³, Y. Houltz⁴, J. Li⁴, O. Janson⁴, H. Nguyen-Thi¹

¹Aix Marseille University, CNRS, IM2NP UMR 7334, 13397, Marseille, France

²BCAST, Brunel University, Uxbridge, Middlesex UB8 3PH, UK

³ACCESS e.V., Intzestrasse 5, 52072 Aachen, Germany

⁴Swedish Space Corporation, P.O. Box 4207, SE-171 04 Solna, Sweden

Keywords: directional solidification, microstructures, gravity level variation, CET

Abstract

In the framework of an ESA-MAP project entitled XRMON, directional solidification experiments of Al – 20 wt% Cu with in situ and real-time X-ray radiography were carried out during Parabolic Flight campaigns. Parabolic flights offer successions of periods with different gravity levels, allowing the investigation of the impact of gravity level variations on the solidification microstructure formation. Directional solidifications of refined Al – 20 wt% Cu alloy were investigated in a dedicated apparatus for a wide range of cooling rates and a constant temperature gradient. X-ray radiography was successfully used to observe the microstructure evolution following the variations of gravity level. During the columnar growth of the refined alloy a sharp increase of gravity level provoked the sudden nucleation of numerous grains ahead of the front. The most potent explanation of this effect is the variation of the liquid undercooling ahead of solid/liquid interface due to the changes of hydrostatic pressure in the melt.

Introduction

Metals properties are strongly related to solidification microstructures and to the accompanying segregation, which are both very sensitive to gravity [1]. Indeed, gravity induces natural convection in the melt due to density variations following the local temperature and concentration [2]. The coupling between fluid flow and solidification has been the subject of a great deal of experimental, theoretical and numerical works. The main conclusion of these studies is that the convection has a significant impact on the solidification process, such as the macroscopic deformation of the solid/liquid interface, macro-segregation in the sample, and the modification of the primary arm spacing. In addition, due to solute rejection during the liquid to solid transition, growing grains and surrounding liquid have generally different densities. Consequently, buoyancy force can act on the solid grains, which lead to their sedimentation or floatation in the liquid phase. Therefore, equiaxed microstructures on Earth and in microgravity are dramatically different. Furthermore, gravity is at the origin of mechanical effects, which can induce the bending of secondary arms when the latter are long enough. In some cases, the bending phenomenon can precede the dendrite fragmentation [3, 4]. Finally, a less common issue

related to gravity is the hydrostatic pressure in the melt. It is well known that hydrostatic pressure applied during solidification significantly reduces the formation of porosities. On the contrary, under microgravity conditions, hydrostatic pressure vanishes and the liquid shape is only determined by the surface tension and the wetting behavior of the melt on solid surfaces. Hence, the loss of hydrostatic pressure in the melt can cause shrinkages or the formation of voids along the sample during microgravity experiments [5]. Therefore, a deeper understanding of gravity effects in solidification microstructure is of great importance for scientists and industrialists alike.

It has long been realized that solidification under microgravity conditions is an efficient way to eliminate most of the buoyancy-related phenomena, providing valuable benchmark data in near-diffusive conditions for the validation of analytical models and numerical simulations. In addition, a comparative study of solidification experiments carried out on Earth and in space can also enlighten the effects of gravity. In this paper, we report experimental results obtained during the 60th ESA-PF (Parabolic Flights) campaign in April 2014. To investigate the impact of gravity level variations on the dynamic of the solidification microstructure formation, it is crucial to achieve in situ and real-time characterization during the solidification experiment. It is now well recognized that X-ray radiography is the method of choice for investigating the solidification front evolution of metallic alloys grown from the melt [6]. In the framework of the ESA-MAP (Microgravity Application Promotion) entitled XRMON (X-ray MONitoring of advanced metallurgical processes under microgravity and terrestrial conditions), a dedicated apparatus named XRMON-GF (Gradient Furnace) was developed to perform directional solidification experiments on Al-based alloys, with in situ X-ray radiography. This facility was successfully used in microgravity conditions onboard MASER-12 sounding rocket in 2012 [7]. In a second step, the XRMON-GF facility was slightly modified to be utilized during parabolic flights. This new facility, entitled XRMON-PFF (Parabolic Flight Facility), was used onboard the Airbus A300 operated by Novespace (www.novespace.fr) to study equiaxed growth of Al – 20 wt% Cu in nearly isothermal conditions [7, 8].

Experiments

Contrary to ISS (International Space Station), satellite and sounding rockets, parabolic flights offer only very short reduced-gravity periods (about 20 seconds) in comparison with typical solidification experiments (several hours). For this reason, the main interest to perform solidification during parabolic flights is to focus on the influence of g-level variations on the growth process. During the 60th ESA-PF campaign, a series of directional solidification experiments on Al – 20 wt% Cu sample was carried out in the XRMON-PFF facility.

XRMON-PFF facility

The XRMON-PFF is shown in Figure 1a in the Airbus A300 Zero-G, with the experimental and control racks. The experimental rack figures three essential components (Figure 1b): the X-ray source, the X-ray detector and the solidification furnace. The furnace is of Bridgman type. A temperature gradient along the sample is imposed by two heaters separated by a gap. The gradient furnace enables directional solidification with thermal gradients within a range of 5-15 K/mm. The heater gap has a “hole” of 5 mm x 5 mm for the X-ray transmission. Solidification is

induced by the power-down method, which consists of applying the same cooling rate R on both heater elements to keep a constant temperature gradient during the process.

A sketch of the X-ray radiography system is presented in Figure 1c. The microfocus X-ray source is a transmission type X-ray tube with a molybdenum target and a $3\ \mu\text{m}$ focal spot. It provides a sufficient photon flux with two peaks of energy at 17.4 keV and 19.6 keV that ensure a good image contrast to study Al-Cu based alloys. The camera system is made of a digital camera with a CCD-sensor adapted for X-ray usage by the integration of a 50 mm thick fiber optical plate that protects the sensor from radiation. A scintillator plate placed in front of the optical fiber converts X-ray radiation to visible spectrum light. As a result of the X-ray beam divergence, a geometric magnification of the object is observed at the detector, which is the ratio of the source-detector to source-object distances; the object in this case being the sample. In this work a magnification of ~ 5 was obtained, for a FOV of about $5 \times 5\ \text{mm}^2$ and an effective pixel size of $\sim 4\ \mu\text{m}$. The acquisition rate is typically 3 frames/s.

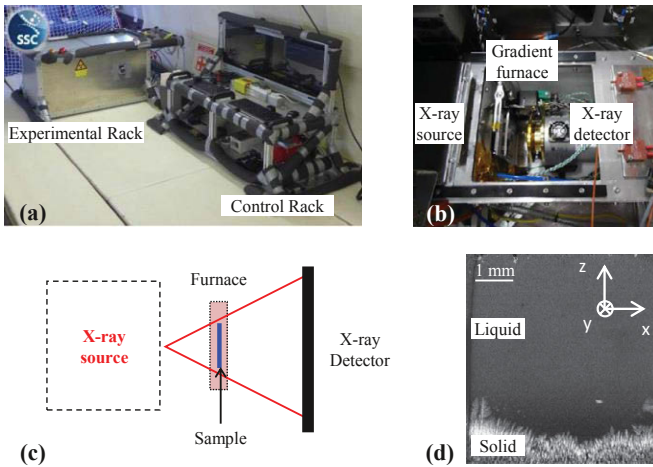


Figure 1. (a) XRMON-Parabolic Flight Facility in Novespace Airbus A300 Zero-G, (b) picture of the solidification furnace and X-ray systems in the experimental rack, (c) sketch of the X-ray radiography system, (d) example of radiograph after image processing.

Variations of grey levels in the radiographs are related to the difference in X-ray absorption of the different parts of the sample, which depends mainly on the local density and composition of the sample. In Al-Cu alloys, copper provides a greater attenuation of the incident X-ray beam than aluminum. Image quality was enhanced by applying an image processing consisting in dividing each frames by a reference picture before cooling starts [9]. After the image processing, radiographs like Figure 1d are obtained, showing the solid-liquid interface during the solidification of Al – 20 wt% Cu. Regions of high copper concentration show up as dark regions in the images, while α -Al dendrites with low copper concentration are discernible as bright regions in the field of view.

Sample preparation

During the 60th ESA-PF campaign, an Al – 20 wt% Cu alloy inoculated with 0.1 wt% AlTiB refiners was investigated in order to determine the solidification conditions that can give rise to a Columnar-to-Equiaxed Transition (CET) [10, 11]. CET is a transition that occurs when equiaxed grains nucleate in the undercooled liquid region ahead of an advancing columnar front. If the number of grains is large enough, they can grow and stop the columnar growth and there is formation of an equiaxed microstructure. AlTiB refiners are used to act as preferential sites for heterogeneous nucleation, and thus to promote the Columnar-to-Equiaxed Transition [12]. The sample dimensions were 50 mm in length, 5 mm in width and 200 to 250 μm in thickness. The sample was placed between stainless steel spacers sandwiched by two glassy carbon sheets sewn together with a silica thread (Figure 2). The crucible was enclosed inside the heaters, having a contact with both sides to achieve the same thermal behavior in microgravity environment as on ground-based experiments.

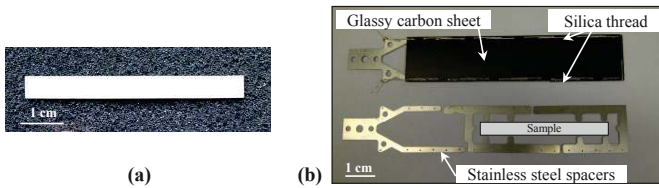


Figure 2. (a) Al – 20 wt% Cu sample and (b) glassy carbon crucible with stainless steel frame, sewn together with a silica thread.

Parabolic flight timeline

According to the parabolic flight trajectory, the gravity level changes during each parabola (Figure 3a) from $1g_0 \rightarrow \sim 1.8g_0 \rightarrow \sim 0g_0 \rightarrow \sim 1.8g_0 \rightarrow 1g_0$, with approximately 24s and 22s at $\sim 1.8g_0$ and $\sim 0g_0$ respectively. During the course of the flight, the parabola is repeated a total of 31 times: a first series of six parabolas, followed by five series of five parabolas with a time interval between two series of 5-8 minutes (Figure 3b).

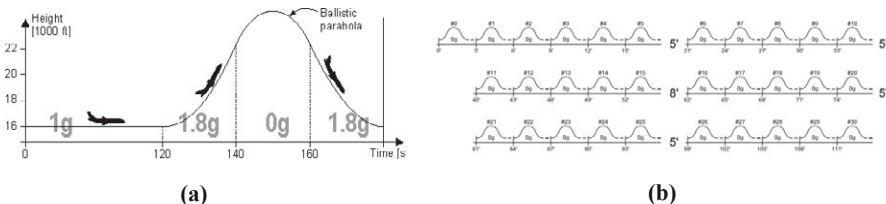


Figure 3. (a) Parabola profile showing the gravity level variation with time, (b) sequence of 31 parabolas during the course of the flight.

Accelerations were recorded for all experiments on three accelerometers on mutually orthogonal axes mounted to the experimental rack. Figure 4 gives typical accelerometer data for five parabolic maneuvers. For a typical maneuver, during low gravity the acceleration on all axes was below $\sim 0.05g_0$. During pullout and climb, the high gravity acceleration parallel to the longitudinal axis of the sample reached $\sim 1.8g_0$ while the accelerations on the two other axes are less than $0.15g_0$. Therefore, we can assume that the gravity vector is always parallel to the sample longitudinal growth axis.

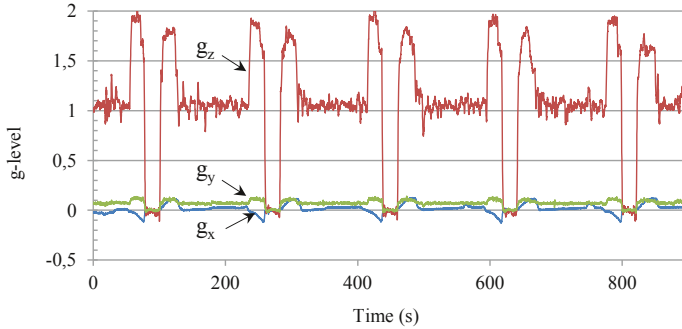


Figure 4. Typical acceleration data during five parabolic maneuvers. The g_z curve is the acceleration parallel to the longitudinal axis of the sample and directed from the top to the bottom of the sample, g_x and g_y curves are the accelerations parallel to the transverse direction of the sample and perpendicular to the main surface of the sample respectively.

Before the beginning of the series of parabolas, the heater temperatures were adjusted to have the solid-liquid interface visible at the bottom in the Field-of-View of the camera, and then kept constant at these temperatures. The cooling of the sample was then triggered a few seconds before the beginning of the first parabola (during the $1g_0$ period), and extended over the whole series of five parabolas (Figure 4). The origin of time ($t = 0s$) was chosen at the beginning of the cooling down. In this paper, we focus on the solidification experiment, at a very slow cooling rate ($R = -0.05$ K/s) and for a temperature gradient ($G = 15$ K/mm).

Results

CET triggering by variation of gravity level

Figure 5 displays a sequence of radiographs recorded during a part of the solidification experiment under varying gravity level. During the $1g_0$ period, the development of a columnar microstructure was observed at the bottom of the Field-of-View (FOV) (white microstructure in Figure 5a). Due to solute rejection during solidification, the liquid just ahead of the columnar front was copper-enriched and appeared darker than the liquid far from the columnar front. Fragmentation phenomena occurred along the solid/liquid interface and the dendrite fragments floated from the bottom to the top due to buoyancy force. Indeed, for this alloy composition (Al – 20 wt% Cu), the dendrite fragments are lighter than the surrounding liquid [7]. During their motion toward the hot region of the sample, the dendrite fragments rapidly melted until their

complete disappearance. Moreover, a few grains nucleated on the crucible wall. Most of them floated toward the top of the sample and melted, but one remained stuck on the crucible wall on the right-hand side of the sample (Figure 5b).

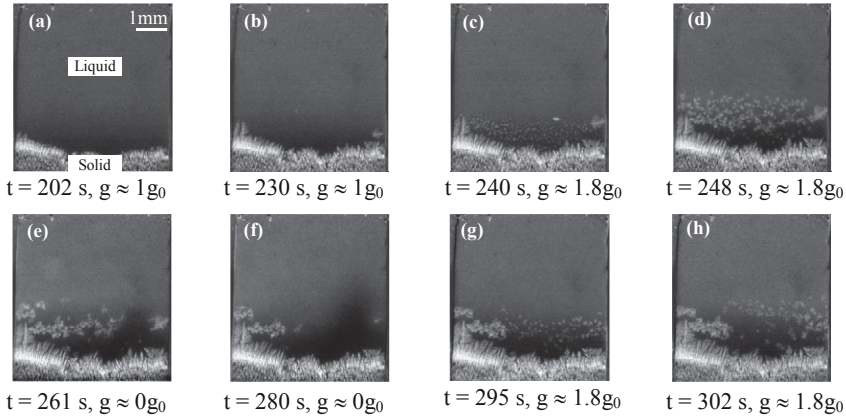


Figure 5. Sequence of radiographs recorded during the solidification of refined Al – 20 wt% Cu, for a cooling rate ($R = -0.05$ K/s), and temperature gradient ($G = 15$ K/mm) during a parabola. The gravity vector is directed vertically downwards relative to the FOV.

When the gravity level suddenly increased from $1g_0$ to $\sim 1.8g_0$ at the beginning of the parabola, a sudden nucleation of a large number of equiaxed grains ahead of the columnar front was observed (Figure 5c). The nucleation rate is about 100 grains/second, which is of the same order of the nucleation rate measured by Murphy for equiaxed growth of a refined Al - 20wt% Cu sample in near-isothermal experiment [8].

This explosive nucleation phase is obviously provoked by the sharp increase of the gravity level. Actually, the grain nucleation event ahead of the columnar front was triggered by an increase of the liquid undercooling ahead of the columnar front. The liquid undercooling at an altitude z is defined as the difference between the liquidus temperature $T_{eq}(z)$ and the real temperature imposed by the temperature gradient $T_L(z)$. If the liquid undercooling reaches the value of the nucleation undercooling of the refining particles, nucleation can occur. The question that rises is: why the liquid undercooling increases when the gravity level augments?

The most potent explanation of this increase of the undercooling is a decrease of the liquid composition ahead of the columnar structure. This composition decrease is attributed to the increase of the hydrostatic pressure of the melt when the gravity level changed from $1g_0$ to $\sim 1.8g_0$. As the two thin glassy carbon sheets are flexible, the hydrostatic pressure rise caused a larger bulging of the sample at the solid-liquid interface, as mentioned by A. Murphy [7]. As a consequence, this bulging increase induced a downward flow of poorer fluid toward the columnar front. Because of the decrease of liquid composition ahead of the columnar front, the local equilibrium temperature augments as well as the constitutional undercooling.

After their nucleation, like dendrite fragments, the new grains started to float and then melted when they reached the hot region of the liquid (Figure 5d and 5e). Some grains remained stuck in the thickness of the sample when their size was too large compared to the sample thickness (Figure 5f). As soon as the gravity level reached $\sim 0g_0$ (Figure 5e), the equiaxed grains stopped moving upward because buoyancy force vanished. During the $0g_0$ period (Figure 5e to Figure 5f), the grains remelted due to an upward copper-enriched fluid flow, which is visible in Figure 4f as a dark region in the liquid ahead of the microstructures. Once again, the origin of this upward fluid flow is related to the vanishing of the hydrostatic pressure and thus the contraction of the crucible during the microgravity period. During the subsequent $\sim 1.8g_0$ period, the explosive nucleation phenomenon occurred again (Figure 5g and 5h). All these phenomena were repeated in the following parabolas. It is worth noting that these observations were also observed in other experiments, with different cooling rates.

Conclusion

X-ray radiography was successfully used during solidification experiments carried out during parabolic flights. It was observed that gravity level variations can have a significant impact on the microstructure formation. The variation of g-level induces a variation of the liquid composition ahead of the solid/liquid interface which affects the constitutional undercooling. In a refined alloy, this undercooling increase can provoke an explosive nucleation of equiaxed grains. Further solidification experiments with different alloy composition are scheduled during future parabolic flight campaigns in the framework of the XRMON project.

Acknowledgments

This study was partly supported by the XRMON project (AO-2004-046) of the MAP program of the European Space Agency (ESA) and by the French National Space Agency (CNES).

References

1. H. Nguyen-Thi, A. Bogno, G. Reinhart, B. Billia, R. H. Mathiesen, G. Zimmermann, Y. Houltz, K. Löth, D. Voss, A. Verga and F. d. Pascale. Investigation of gravity effects on solidification of binary alloys with in situ X-ray radiography on earth and in microgravity environment. *Journal of Physics: Conference Series* 2011;327:012012
2. D. T. J. Hurle. *Interactive Dynamics of Convection and Solidification* 1992
3. G. Reinhart, H. Nguyen-Thi, N. Mangelinck-Noel, J. Baruchel and B. Billia. In Situ Investigation of Dendrite Deformation During Upward Solidification of Al-7wt.%Si. *JOM* 2014;66:1408-1414
4. G. Reinhart, A. Buffet, H. Nguyen-Thi, B. Billia, H. Jung, N. Mangelinck-Noel, N. Bergeon, T. Schenk, J. Hartwig and J. Baruchel. In-Situ and real-time analysis of the formation of strains and microstructure defects during solidification of Al-3.5 wt pct Ni alloys. *Metallurgical and Materials Transactions a-Physical Metallurgy and Materials Science* 2008;39A:865-874

5. B. Drevet, D. Camel, C. Malmejac, J. J. Favier, H. Nguyen Thi, Q. Li and B. Billia. Cellular and Dendritic Solidification of Al-Li Alloys during the D2-Mission. *Adv. In Space Res.* 1995;16:173-176
6. H. Nguyen-Thi, L. Salvo, R. H. Mathiesen, L. Arnberg, B. Billia, M. Suery and G. Reinhart. On the interest of synchrotron X-ray imaging for the study of solidification in metallic alloys. *Comptes Rendus Physique* 2012;13:237-245
7. H. Nguyen-Thi, G. Reinhart, G. Salloum-Abou-Jaoude, D. J. Browne, A. G. Murphy, Y. Houltz, J. Li, D. Voss, A. Verga, R. H. Mathiesen and G. Zimmermann. XRMON-GF Experiments Devoted to the in Situ X-ray Radiographic Observation of Growth Process in Microgravity Conditions. *Microgravity Science and Technology* 2014;26:37-50
8. A. G. Murphy, J. Li, O. Janson, A. Verga and D. J. Browne. Microgravity and Hypergravity Observations of Equiaxed Solidification of Al-Cu Alloys using In-situ X-radiography recorded in Real-time on board a Parabolic Flight. *Materials Science Forum* 2014;790-791:52-58
9. H. Nguyen-Thi, G. Reinhart, G. S. Abou Jaoude, R. H. Mathiesen, G. Zimmermann, Y. Houltz, D. Voss, A. Verga, D. J. Browne and A. G. Murphy. XRMON-GF: A novel facility for solidification of metallic alloys with in situ and time-resolved X-ray radiographic characterization in microgravity conditions. *Journal of Crystal Growth* 2013;374:23-30
10. H. Nguyen Thi, G. Reinhart, N. Mangelinck-Noël, H. Jung, B. Billia, T. Schenk, J. Gastaldi, J. Härtwig and J. Baruchel. In-Situ and Real-Time Investigation of Columnar to Equiaxed Transition in Metallic Alloy. *Metall. Mater. Trans. A* 2007;38-7:1458-1464
11. G. Reinhart, N. Mangelinck-Noël, H. Nguyen Thi, T. Schenk, J. Gastaldi, B. Billia, P. Pino, J. Härtwig and J. Baruchel. Investigation of Columnar-Equiaxed Transition and Equiaxed growth of Aluminium Based Alloys by X-Ray Radiography. *Materials Science and Engineering A* 2005;413-414:384-388
12. G. Reinhart, H. Nguyen-Thi, N. Mangelinck-Noël, T. Schenk, B. Billia, J. Gastaldi, J. Härtwig and J. Baruchel. In-situ observation of transition from columnar to equiaxed growth in Al-3.5 wt% Ni alloys by synchrotron radiography. *Modeling of Casting, Welding and Advanced Solidification Processes* 2006;XI:359-366